FEBS Letters 557 (2004) 174–180 FEBS 28000

Biophysical characterization of hepatitis C virus core protein: implications for interactions within the virus and host

Meghan Kunkel, Stanley J. Watowich*

Department of Human Biological Chemistry and Genetics and the Sealy Center for Structural Biology, University of Texas Medical Branch, Galveston, TX 77555, USA

Received 12 November 2003; revised 8 December 2003; accepted 10 December 2003

First published online 24 December 2003

Edited by Thomas L. James

Abstract A primary function of the hepatitis C virus (HCV) core protein is to package the viral genome within a nucleocapsid. In addition, core protein has been shown to interact with more than a dozen cellular proteins, and these interactions have been suggested to play critical roles in HCV pathogenesis. A more complete knowledge of the biophysical properties of the core protein may help to clarify its role in HCV pathogenesis and nucleocapsid assembly and provide a basis for the development of novel anti-HCV therapies. Here we report that recombinant mature core protein exists as a large multimer in solution under physiological conditions. Far-UV circular dichroism (CD) experiments showed that the mature core protein contains stable secondary structure. Studies with truncated core protein demonstrated that the C-terminal region of the core protein is critical for its folding and oligomerization. Intrinsic fluorescence spectroscopy and near-UV CD analysis indicated that the tryptophan-rich region (residues 76–113) is largely solvent-exposed and not likely responsible for multimerization of the mature core protein in vitro.

Key words: Core protein; Protein biophysics; Hepatitis C virus

1. Introduction

Although hepatitis C virus (HCV; family Flaviviridae) is a major cause of chronic hepatitis, cirrhosis, and hepatocellular carcinoma, there are currently no satisfactory treatments for HCV infection [1,2]. Sequence similarities between HCV core protein and other viral capsid proteins, and studies of infectious sera, suggest that a primary function of the core protein is to package the viral genome within a nucleocapsid [3,4]. There is also growing evidence that the core protein plays a critical role in HCV pathogenesis. Core protein has been reported to interact with over a dozen cellular proteins, thereby impacting immune presentation, apoptosis, cell transformation, lipid metabolism, and transcription (see [5] and references therein). However, difficulties in obtaining purified mature core protein have in many instances required that core proteins with extensive C-terminal deletions be used for in vitro functional studies. In addition, lack of a model system that reproduces HCV replication and pathogenesis has hindered correlating in vitro observations with in vivo pathogenesis. These factors have led to differing conclusions about the role of the core protein in HCV-mediated liver disease. Despite accumulating evidence of its multifunctional nature, little is known about the biophysical properties of the core protein. Information about the structure and association state of the core protein could reveal features that provide a basis for its apparent multiplicity of function, help to explain disparate results obtained from different systems or techniques, and provide important information for the design of novel HCV therapies.

2. Materials and methods

2.1. Determination of protein parameters

Molecular weights, extinction coefficients, and theoretical isoelectric points were determined using the ProtParam program of the Expert Protein Analysis System (ExPASy) proteomics server of the Swiss Institute of Bioinformatics [6]. Protein concentrations were determined by UV spectrophotometry at a wavelength of 280 nm in 6 M guanidine hydrochloride solution, using extinction coefficients of 40 660 M^{-1} cm^{-1} for HCVC 179 and 37 980 M^{-1} cm^{-1} for HCVC 124. Molecular weights, calculated from the sequence of each protein minus the N-terminal Met, were 19 523 Da for HCVC 179 and 13 960 Da for HCVC 124.

2.2. Reduction of disulfide bonds

To examine the proteins under reducing conditions, each protein was first denatured in 6 M guanidine hydrochloride and 10 mM dithiothreitol (DTT) for 24 h and then extensively dialyzed into the refolding buffer, 20 mM Tris (pH 7.0), 150 mM NaCl, 10 mM DTT, at 4°C.

2.3. Analytical ultracentrifugation

Sedimentation velocity and sedimentation equilibrium studies were carried out at 4°C in a Beckman Optima XL-A analytical ultracentrifuge (Beckman Coulter, Fullerton, CA, USA) fitted with an An-60Ti rotor and absorption optics. Samples were prepared at concentrations of 0.1–2 mg/ml, dialyzed overnight in 20 mM Tris, 150 mM NaCl (pH 7.0), and clarified by a 20 min spin at 16 000 × *g* at 4°C prior to the experiments. Data were collected at a wavelength of 280 nm. Sedimentation velocity measurements were made with rotation speeds of 20 000 rpm for HCVC 179 and 45 000 rpm for HCVC 124 and data collected at 4°C. Absorbance scans were collected at intervals of 1 min, and at least 100 scans were recorded per sample. Spectra were analyzed with DCDT+ Version 1.13 software [7] and the web analysis program SEDFIT [8]. Measured sedimentation coefficient (S) values were expressed as $s^*_{20,W}$. Partial specific volumes, buffer density, buffer viscosity, and temperature corrections were determined using the protein analysis software SedNTerp (University of New Hampshire, Durham, NH, USA). Sedimentation equilibrium measurements were made with rotation speeds of 9000 rpm for HCVC 179 and 21 000 rpm for HCVC 124 and data collected at 4°C. Spectra

*Corresponding author. Fax: (1)-409-747 4745.
E-mail address: watowich@bloch.utmb.edu (S.J. Watowich).

Abbreviations: HCV, hepatitis C virus; CD, circular dichroism; S, sedimentation coefficient; DTT, dithiothreitol

0014-5793/03/$30.00 © 2003 Published by Elsevier B.V. on behalf of the Federation of European Biochemical Societies.
doi:10.1016/S0014-5793(03)01486-8

were analyzed with Microcal Origin software (Beckman). Samples were allowed to achieve sedimentation equilibrium over the course of 24 h and were judged to be at equilibrium when sequential scans 2 h apart were superimposable.

2.4. Electron microscopy

HCVC 179 in neutral buffer was adsorbed to 400 mesh carbon-Formvar grids and stained with 2% uranyl acetate. Micrographs were captured on a Philips EM201 with an acceleration voltage of 60 kV and at a magnification of ×94 000.

2.5. Circular dichroism spectroscopy

Circular dichroism (CD) measurements were recorded on an Aviv 62DS CD spectrophotometer (Aviv Instruments, Lakewood, NJ, USA) at 25°C, using 0.1 cm path length cuvettes. Samples were prepared with concentrations of 0.4–2 mg/ml for HCVC 179 and 0.3–3 mg/ml for HCVC 124 in 20 mM Tris, 150 mM NaCl (pH 7.0). Far-UV spectra were collected from 200 to 250 nm, and near-UV spectra were collected from 250 to 310 nm. High solvent absorbance, monitored by dynavoltages that exceeded 400 V, prevented the collection of data below 200 nm. Spectra were acquired by averaging three scans. Buffer absorbances were collected simultaneously and subtracted from each sample measurement. Scans were smoothed using software provided by the instrument manufacturer. Far-UV CD values were reported as mean residue ellipticity, $[\theta]_{MRW}$, with units of deg cm^2 dmol^{-1}. Near-UV CD values were reported as decadic molar CD, $\Delta\varepsilon$, with units of M^{-1} cm^{-1}. Secondary structure content for HCVC 179 was estimated by deconvolution of the recorded spectrum into reference helix, sheet, turn, and coil spectra using regression analysis within the program Mathematica [9].

2.6. Intrinsic fluorescence spectroscopy

Fluorescence measurements were carried out in 1 cm path length cuvettes on an SPEX FluoroMax (Jobin Yvon Horiba, Edison, NJ, USA) at 25°C, using dM3000 software supplied by the manufacturer (JY Horiba). Samples were prepared at concentrations of 0.2 mg/ml for HCVC 179 and 0.14 mg/ml for HCVC 124 in 20 mM Tris, 150 mM NaCl (pH 7.0). Denaturing conditions included 6 M guanidine hydrochloride in the sample buffer. Tryptophan intrinsic fluorescence was monitored using an excitation wavelength of 295 nm and an emission wavelength range between 300 and 410 nm. Spectra were acquired by averaging three scans collected at a rate of 1 nm/s. Buffer absorbance was collected and subtracted from each sample measurement. Relative intensity values were normalized to L-tryptophan fluorescence.

3. Results

3.1. HCVC 179 associated as a large homogeneous multimer; HCVC 124 was primarily a monomer

To determine the oligomeric state of the core proteins in solution, purified recombinant proteins HCVC 179 and HCVC 124 were analyzed by analytical ultracentrifugation. HCVC 179 (aa 1–179) represents the mature core protein product of post-translational cleavage [4,10–13], and HCVC 124 (aa 1–124) is a C-terminally truncated core protein that includes regions previously implicated in RNA binding and self-association of the core protein [12,14,15]. Expression and purification procedures have been described previously [16].

Time derivative analysis [7] of HCVC 179 velocity sedimentation data could be fit best to a model of one species, with a sedimentation coefficient of 11S (Fig. 1A). Van Holde–Weischet analysis [8,17], which effectively removes the contribution of diffusion, indicated that the oligomers were monodisperse and homogeneous with a sedimentation value of ∼11S (Fig. 2). Data from sedimentation equilibrium ultracentrifugation of HCVC 179 were well described by a model of a single homogeneous species (Fig. 3A). The single species model predicts the observed species has an average molecular mass of ∼500 kDa, which strongly suggests that HCVC 179 self-associated as a multimer of ∼24–26 core monomers, with each monomer at a molecular mass of ∼20 kDa. Sedimentation equilibrium data for HCVC 179 under reducing conditions of 2 mM DTT were also well described by a model of a single homogeneous species, with an average molecular mass

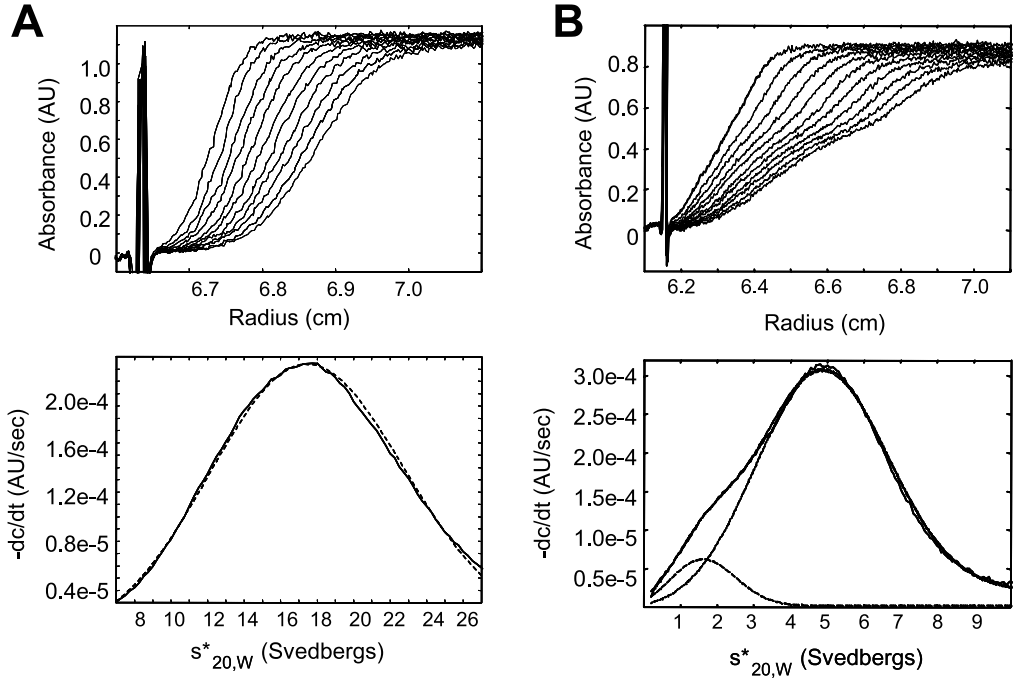

Fig. 1. Characterization of the oligomeric state of HCVC 179 (A) and HCVC 124 (B) by sedimentation velocity. The sedimentation profile is shown in the top panels; the bottom panel show the time derivative $-dc/dt$ analysis with the distribution of $-dc/dt$ as a function of the sedimentation coefficient. The dashed lines of the model are overlaid on the solid lines of the experimental data. Measured S values were expressed as $s^*_{20,W}$. Measurements were made with rotation speeds of 20 000 rpm for HCVC 179 and 45 000 rpm for HCVC 124 at 4°C.

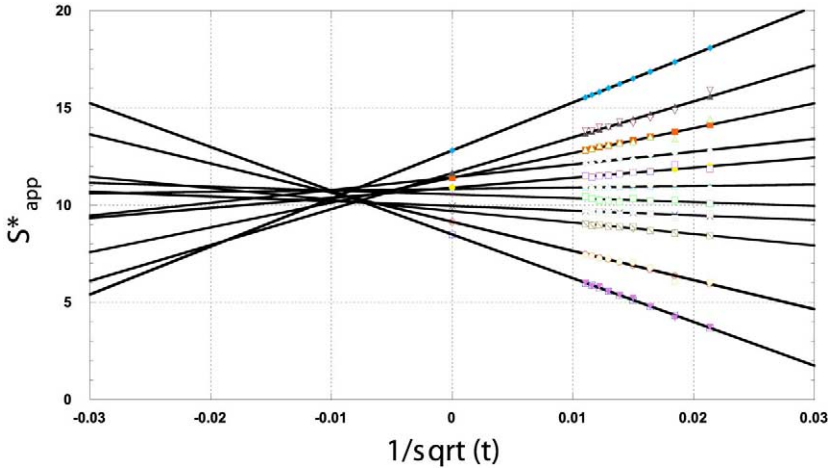

Fig. 2. Van Holde–Weischet analysis of velocity sedimentation data for HCVC 179. The sedimenting boundary of HCVC 179 was divided into 10 fractions by the program SEDFIT [8]. The graph shows the apparent sedimentation coefficient (s^*_{app}) distribution determined for each fraction plotted against the inverse of the square root of time, extrapolated to infinite time.

of ~500 kDa (data not shown). Attempts to fit the data to equilibrium models of association containing multiple species were unsuccessful as shown by increased variance and unrealistic values for equilibrium constants. Changes in protein concentration from 0.2 to 2 mg/ml did not significantly modify the sedimentation profile of HCVC 179 (data not shown).

When compared to typical globular complexes, the sedimentation coefficient of HCVC 179 is notably small in relation to its molecular mass (e.g. catalase, $M = 250$ kDa, 11.3S, urease, $M = 483$ kDa, 18.6S). This indicates that HCVC 179 is likely asymmetric in shape, which gives it a high frictional coefficient and reduces its S value. In accordance with the ultracentrifugation data, negative stain electron microscopy of HCVC 179 revealed a homogeneous population of uniformly sized particles, with diameters of ~15 nm (Fig. 4). We therefore concluded that the 11S multimer was the predominant solution state of HCVC 179 and that this large species was not in equilibrium with other species.

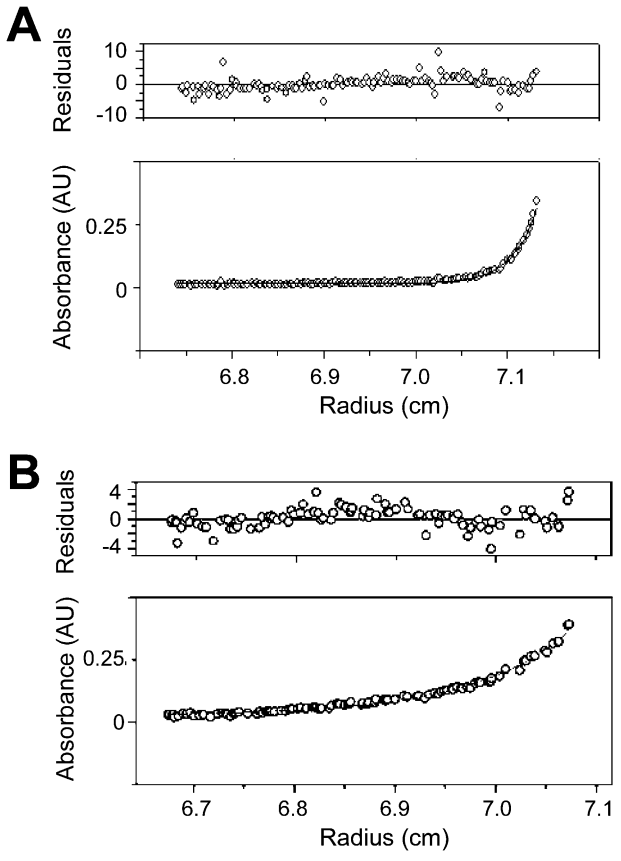

Fig. 3. Equilibrium sedimentation of HCVC 179 and HCVC 124. The distribution of residuals is shown at the top, and the bottom panel shows the absorbance versus radial exponential distribution of the HCVC proteins. A: The data were collected at 9000 rpm, 4°C. The curve is the theoretical distribution of a ~500,000 Da oligomer. B: The data were collected at 21 000 rpm, 4°C. The curve represents a mixture of monomeric and dimeric species, with an average molecular mass of ~25 000 Da.

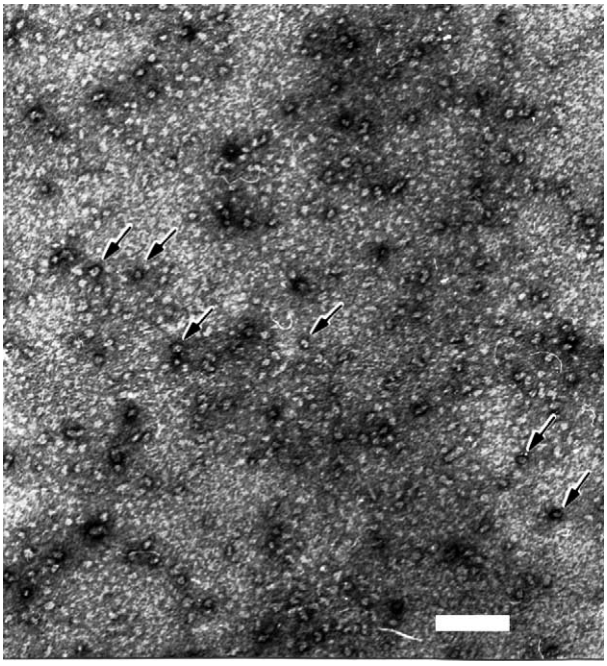

Fig. 4. Negative stain electron microscopy of HCVC 179. Representative 11S cores are identified with arrows, and the white bar corresponds to 100 nm.

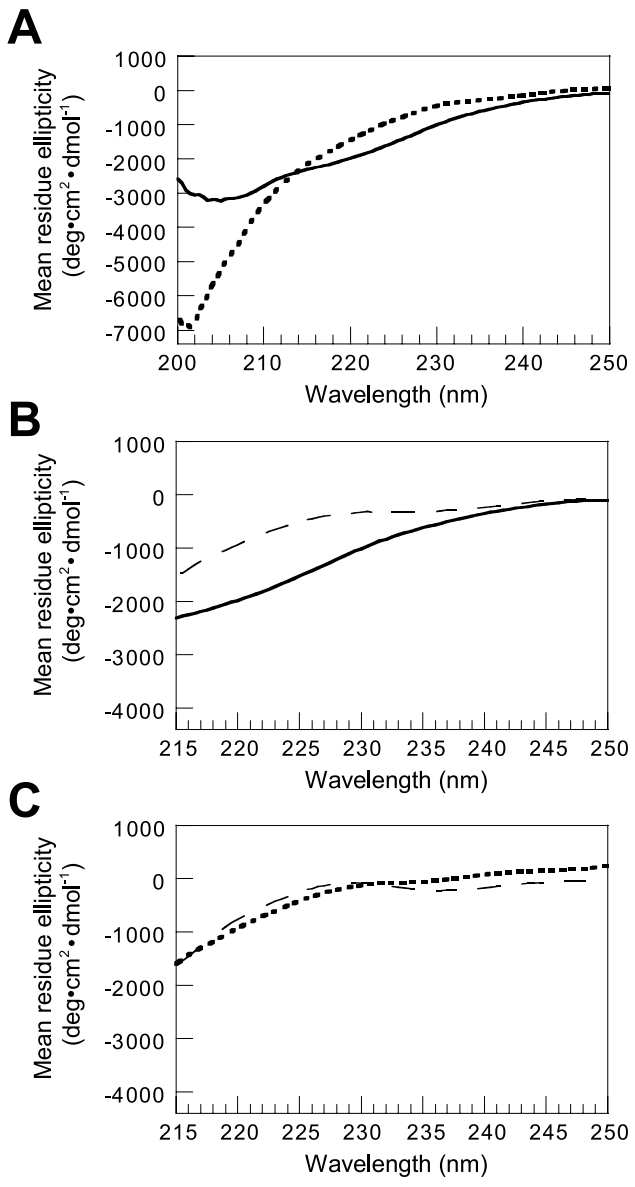

Fig. 5. Far-UV CD spectroscopy of HCVC 179 and HCVC 124 under neutral and denaturing conditions. Ellipticity values were averaged over the total number of amino acid residues in order to directly compare the two proteins. A: HCVC 179 (solid line) and HCVC 124 (dotted line) under neutral conditions of 10 mM K-phosphate, 50 mM KSO_4 (pH 7.0). B: HCVC 179 under neutral conditions (solid line) and in 6 M urea (dashed line). C: HCVC 124 under neutral conditions (dotted line) and in 6 M urea (dashed line). The spectra in B and C were truncated at 215 nm, since the dynavoltage exceeded 400 V due to high solvent absorbance, and thus data above 215 nm were considered unreliable.

In contrast to HCVC 179, analytical ultracentrifugation of HCVC 124 did reflect a slight concentration dependence and a change in the state of multimerization upon the addition of reducing agent. Time derivative analysis of velocity sedimentation data of HCVC 124 indicated that the protein consisted of two sedimenting forms of 1.1S and 3.5S (Fig. 1B). The 3.5S form was the major species of HCVC 124, representing $>80\%$ of the sample absorbance. At lower protein concentrations of 0.1–0.3 mg/ml, time derivative analysis indicated the presence of a small proportion of the 1.1S species in addition to the 3.5S species, but upon increasing protein concentration, the spectrum reflected the larger 3.5S form only (data not shown). Equilibrium sedimentation of HCVC 124 indicated that these species represented a mixture of monomer and dimer, with an average molecular mass of $\sim$25 kDa (Fig. 3B). However, in the presence of 2 mM DTT (data not shown), the protein was completely reduced to the monomeric species, with an average molecular mass of $\sim$14 kDa. Since there is only one cysteine residue present in HCVC 124 (at position 91), it is not possible that the 3.5S species was a non-covalent dimer stabilized by intramolecular disulfide bonds. Instead, the ultracentrifugation analysis definitively showed that the dimerization of HCVC 124 was a result of an intermolecular disulfide bond linkage, and that HCVC 124 is likely monomeric in the reducing environment of a cell.

3.2. HCVC 179 contained stable secondary structure

To investigate the folded state of HCV core protein, HCVC 179 and HCVC 124 were analyzed by far-UV CD spectroscopy under physiological conditions (Fig. 5A). HCVC 179 appeared to contain stable secondary structure, as shown by a distinct minimum in the spectra at 208 nm, a trough between 210 and 220 nm, and a crossover point at 198 nm. Regression analysis of the CD spectrum [9], using a deconvolution of reference helix, sheet, turn, and random coil spectra, indicated the following distribution of secondary structure: 16% α-helix, 29% β-sheet and turns, and 55% random coil. In contrast, the spectrum of HCVC 124 showed only a marked depression in the region of 200 nm and had no crossover point, which is characteristic of an unordered protein [17]. These spectra were compared to spectra of each protein under denaturing conditions. The spectrum of HCVC 179 denatured in 6 M urea (Fig. 5B) clearly departed from the spectrum of HCVC 179 under physiological conditions, whereas the spectrum of HCVC 124 denatured in 6 M urea (Fig. 5C) was virtually superimposable on that of HCVC 124 under physiological conditions.

3.3. Tryptophan residues were largely solvent-exposed

The six tryptophan residues of the core protein are located at positions 76, 83, 93, 96, 107, and 113, with all but Trp 113 conserved in all HCV isolates [18]. This region has been implicated as part of the sequence involved in self-association of the core protein [14,15]. Since this region is present in both the monomeric HCVC 124 and the multimeric HCVC 179, we examined the intrinsic fluorescence of HCVC 179 and HCVC 124 to gain insight into the structure and environment of the region around residues 76–113. If this were the region responsible for the self-association of the core protein, a significant difference in the spectra of the two proteins would be expected: HCVC 124 should reflect a hydrophilic (solvent-exposed) environment of its tryptophans like that under denaturing conditions, with a λ_{max} approaching 355 nm, and HCVC 179 should reflect a hydrophobic environment, quenched through the interaction with other core proteins, with a λ_{max} approaching 310 nm.

Equimolar solutions of HCVC 179 and HCVC 124 were irradiated at an excitation wavelength of 295 nm to ensure that only tryptophan residues were excited during these experiments. The fluorescence emission spectrum of HCVC 179 consisted of a peak centered at 341 nm, while the emission spectrum of HCVC 124 consisted of a peak at 346 nm (Fig. 6A). These results were consistent with largely solvent-ex-

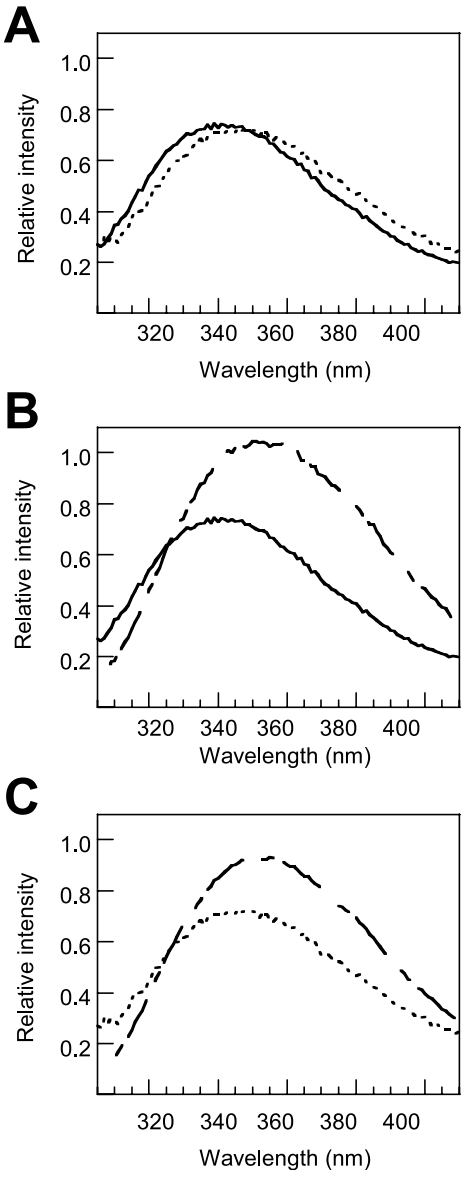

Fig. 6. Intrinsic fluorescence emission of HCVC 179 and HCVC 124. A: HCVC 179 (solid line) and HCVC 124 (dotted line) under neutral conditions of 20 mM Tris, 150 mM NaCl (pH 7.0) with $\lambda_{max} = 341$ for HCVC 179 and $\lambda_{max} = 346$ for HCVC 124. B: HCVC 179 under neutral conditions (solid line) and in 6 M guanidine HCl (dashed line). C: HCVC 124 under neutral conditions (dotted line) and in 6 M guanidine HCl (dashed line).

posed tryptophans in both HCVC 124 and HCVC 179. The λ_{max} of the emission spectra of both HCVC 179 and HCVC 124 in physiological buffers was blue shifted (decreased) relative to λ_{max} of their emission spectra in 6 M guanidine hydrochloride denaturing buffer (Fig. 6B,C). The blue shift was greater for HCVC 179 (Fig. 5B) than for HCVC 124 (Fig. 6C). The addition of 10 mM DTT under physiological conditions did not alter the spectrum of HCVC 179 and slightly broadened the λ_{max} of the emission spectra of HCVC 124 (data not shown). These results indicated that the blue shifts seen in the proteins under native conditions were not due to a shielding of the tryptophans by disulfide bonds at cysteines near the tryptophan-rich region (i.e. Cys 91 or Cys 128). Instead, these blue shifts implied that the tryptophans were in a more hydrophobic environment under physiological conditions. The more hydrophobic tryptophan local environment in HCVC 179 could result from additional structure in HCVC 179, relative to HCVC 124, or from the multimerization of HCVC 179.

To further probe for conformational constraints among the aromatic residues, HCVC 179 and HCVC 124 were analyzed by near-UV CD spectroscopy under physiological conditions. Under reducing conditions, HCVC 124 and HCVC 179 showed nearly identical CD signals in the near-UV region (Fig. 7A). The positive peak at 280 nm and the shoulder at 265–275 nm in the CD spectra indicated the presence of some

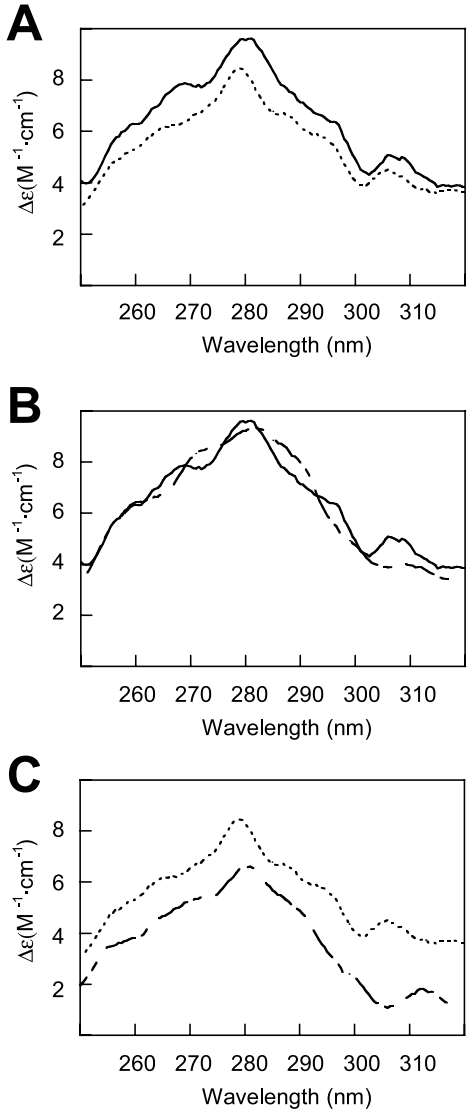

Fig. 7. Near-UV CD spectroscopy of HCVC 179 and HCVC 124. CD spectra are reported as decadic molar CD. Averaging intensities over the total number of amino acid residues is not justified, since only Trp, Tyr, Phe, and Cys contribute CD to this region. HCVC 179 (solid line) and HCVC 124 (dotted line) were analyzed in the presence of 10 mM DTT in order to eliminate any contribution of disulfide bonds to the CD signal. A: HCVC 179 (solid line) and HCVC 124 (dotted line) under neutral conditions of 20 mM Tris 150 mM NaCl (pH 7.0). B: HCVC 179 under neutral conditions (solid line) and in 6 M guanidine HCl (dashed line). C: HCVC 124 under neutral conditions (dotted line) and in 6 M guanidine HCl (dashed line).

conformational constraints involving tyrosines, and the broad shoulder at 290–300 nm indicated some conformational constraints of tryptophans [19]. The near-UV CD signals for both core proteins did not change significantly under denaturing conditions (Fig. 7B,C). Under the conditions of 6 M guanidine hydrochloride with 10 mM DTT, HCVC 179 lost its secondary structure as well as it ability to multimerize. These near-UV CD results then indicated that structural changes that occurred in the transition between monomeric and multimeric states did not affect the environment of the aromatic residues. This suggested that the CD signal in the near-UV region resulted from conformational constraints that arose from linear hydrophobic clustering as opposed to tertiary interaction.

4. Discussion

This biophysical characterization of the core protein indicated that the C-terminal residues 125–179 were critical for the folding and oligomerization of the core protein. The mature core protein contained significant secondary structure and associated as a large multimer of ~24 monomers, while C-terminally truncated core protein was unstructured and monomeric. Additionally, the tryptophan-rich region, previously shown to facilitate self-association in yeast two-hybrid experiments, was not responsible for this interaction in vitro. Since the tryptophans were largely solvent-exposed, and this region did not undergo significant changes in tertiary interaction upon multimerization, it is unlikely the tryptophan-rich region is the major interface for core–core interactions in vitro.

Our results may help clarify some experimental results concerning core protein and its reported interactions with multiple cellular proteins. In many of these studies, C-terminal deletion core proteins (residues 1 to ~101–124, depending on the study) were used to detect in vivo interactions with cellular proteins since these constructs were more soluble than the full-length core protein [5]. However, based on our biophysical results, the C-terminal deletion core proteins would likely have been unstructured and monomeric, while the mature core protein would be structured and multimeric. The strikingly different biophysical profile of the C-terminally truncated core from that of the mature core protein implies that it may interact with viral and host cell factors differently than the mature core protein. The lack of structure in C-terminally truncated core suggests that it is likely to recognize host macromolecules through sequence-specific interactions while structured non-contiguous epitopes may regulate mature core protein interactions with host proteins.

It is also possible that the C-terminal deletion core proteins used to investigate host cell interactions became structured through their interaction with nucleic acid. The role that binding to nucleic acid and/or intracellular membranes may play in the folding and assembly of the core protein should be kept in mind. We have previously shown that free unstructured HCVC 124 adopts a stable conformation upon binding to heterologous nucleic acid and that RNA is required for the in vitro assembly of HCV core protein [16,20]. Since the core protein non-specifically binds nucleic acid in vitro [21,22], it is likely that core protein is associated with nucleic acid in cell culture. Thus, it is possible that the binding of nucleic acid to the core protein has influenced the reported interactions between the C-terminal deletion core proteins and host cell proteins or the multimerization of core protein in cell based systems [14,15].

Finally, the role of the multimeric state of the mature core protein is unknown. The formation of the 11S species of core protein may be an intermediate in the assembly pathway. The accumulation of core protein at the site of assembly may accelerate the formation of the capsid shell and decrease the number of additional interactions that the core protein must make upon assembly, thereby increasing the efficiency of the reaction. However, results from self-assembly of the 11S core protein into nucleocapsid-like particles imply that additional interactions or steps are likely required for the 11S core proteins to form particles consistent with the morphology and size of nucleocapsids from infectious viruses [16]. Nucleocapsids have not been observed in the cytoplasm for any member of the Flaviviridae family, indicating that an association with an intracellular membrane may be critical for the assembly of the particle in vivo.

The formation of the 11S core may also be critical for an association with lipid droplets. A study of this association indicated that deletions of core sequence between residues 125 and 154 disrupted the core–lipid droplet interaction [23]. These deletions correlated with a reduced stability of the core protein, and occur with the region of the protein necessary for formation of a structured molecule. It is possible that the core protein must be structured and oligomeric in order to make an association with lipid droplets. Deletion of core residues 161–166 also disrupted the core–lipid droplet interaction [23]; these residues likely do not disrupt the core structure but may form the core binding epitope. Finally, the 11S core may also facilitate interactions between cellular and viral factors by acting as a scaffold for promoting protein–protein contacts.

Acknowledgements: This work was supported by a pilot project grant (S.W.) under the Hepatitis C Cooperative Research Center Grant U19-AI0035 from the National Institutes for Allergy and Infectious Diseases, a fellowship from a National Institutes of Health Training Grant on Emerging and Tropical Infectious Diseases (M.K.), a James W. McLaughlin predoctoral fellowship (M.K.), and the Sealy Center for Structural Biology (University of Texas Medical Branch). We thank Dr. S. Lemon for helpful discussions, Dr. C. Chin for assistance with the analytical ultracentrifugation experiments, L. Lee and Dr. J. Lee for assistance with circular dichroism measurements and critical reading of the manuscript, Dr. V. Popov for assistance with electron microscopy, Marta Lorinczi for technical assistance, and Dr. R. Fox for access to the spectrofluorometer.

References

[1] Francki, R.I.B., Fauquet, C.M., Knudson, D.L. and Brown, F. (1991) in: Archives of Virology, Suppl. 2, Springer-Verlag, New York.
[2] Lemon, S.M. and Brown, E.A. (1995) in: Principles and Practices of Infectious Diseases, 4th ed. (Madnell, G.L., J.E.B. and Dolin, R., Eds.), pp. 1474–1486, Churchill Livingstone, New York.
[3] Kato, N., Hijikata, M., Ootsuyama, Y., Nakagawa, M., Ohkoshi, S., Sugimura, T. and Shimotohno, K. (1990) Proc. Natl. Acad. Sci. USA 87, 9524–9528.
[4] Yasui, K. et al. (1998) J. Virol. 72, 6048–6055.
[5] McLauchlan, J. (2000) J. Viral Hepat. 7, 2–14.
[6] Appel, R.D., Bairoch, A. and Hochstrasser, D.F. (1994) Trends Biochem. Sci. 19, 258–260.
[7] Philo, J.S. (2000) Anal. Biochem. 279, 151–163.
[8] Schuck, P. (2000) Biophys. J. 78, 1606–1619.
[9] Wolfram, S. (1996) The Mathematica Book, 3rd ed., Wolfram Media and Cambridge University Press, Champaign, IL.

[10] Hussy, P., Langen, H., Mous, J. and Jacobsen, H. (1996) Virology 224, 93–104.
[11] Lo, S.Y., Masiarz, F., Hwang, S.B., Lai, M.M. and Ou, J.H. (1995) Virology 213, 455–461.
[12] Santolini, E., Migliaccio, G. and La Monica, N. (1994) J. Virol. 68, 3631–3641.
[13] Selby, M.J. et al. (1993) J. Gen. Virol. 74, 1103–1113.
[14] Matsumoto, M., Hwang, S.B., Jeng, K.S., Zhu, N. and Lai, M.M. (1996) Virology 218, 43–51.
[15] Nolandt, O., Kern, V., Muller, H., Pfaff, E., Theilmann, L., Welker, R. and Krausslich, H.G. (1997) J. Gen. Virol. 78, 1331–1340.
[16] Kunkel, M., Lorinczi, M., Rijnbrand, R., Lemon, S.M. and Watowich, S.J. (2001) J. Virol. 75, 2119–2129.
[17] Van Holde, K.E. and Weischet, W.O. (1975) Biopolymers 17, 1387–1403.
[18] Bukh, J., Purcell, R.H. and Miller, R.H. (1994) Proc. Natl. Acad. Sci. USA 91, 8239–8243.
[19] Strickland, E.H. (1974) CRC Crit. Rev. Biochem. 2, 113–175.
[20] Kunkel, M. and Watowich, S.J. (2002) Virology 294, 239–245.
[21] Fan, Z., Yang, Q.R., Twu, J.S. and Sherker, A.H. (1999) J. Med. Virol. 59, 131–134.
[22] Tanaka, Y., Shimoike, T., Ishii, K., Suzuki, R., Suzuki, T., Ushijima, H., Matsuura, Y. and Miyamura, T. (2000) Virology 270, 229–236.
[23] Hope, R.G. and McLauchlan, J. (2000) J. Gen. Virol. 81, 1913–1925.